Desalination and Water Treatment
www.deswater.com

doi: 10.5004/dwt.2017.20836

77 (2017) 377–386
May

High-efficient capture of C.I. Basic Blue 3 by carboxymethyl-β-cyclodextrin conjugated magnetic composite

Baowei Hu[a,*], Qingyuan Hu[b], Jun Hu[c,d], Chengguang Chen[b]

[a]*School of Life Science, Shaoxing University, Huancheng West Road 508, Shaoxing 312000, China, Tel./Fax: +86-575-88341820; emails: baoweihusxu@sina.cn, hbw@usx.edu.cn*
[b]*Department of Architectural Engineering for Shaoxing University Yuanpei College, Shaoxing 312000, China, emails: qingyuanhusxu@sina.cn (Q. Hu), chengguangchensxu@163.com (C. Chen)*
[c]*School of Electronic Engineering, Dongguan University of Technology, Dongguan 523808, China, email: junhudongguan@126.com*
[d]*NAAM Research Group, Faculty of Science, King Abdulaziz University, Jeddah 21589, Saudi Arabia*

Received 1 November 2016; Accepted 2 May 2017

ABSTRACT

In the present study, carboxymethyl-β-cyclodextrin (CM-CD) molecules were introduced onto the surfaces of Fe_3O_4 nanoparticles via chemical co-precipitation approach. The synthesized Fe_3O_4/CM-CD composite exhibited high magnetism and could be easily separated from the aqueous phase by exposing to an external magnetic field. In addition, the composite was stable in solution over a wide pH range. The effects of contact time, solution pH, ionic strength, solid dosage and temperature on the removal performance of Fe_3O_4/CM-CD toward a cationic dye named C.I. Basic Blue 3 (BB3) were evaluated by using the batch technique. The sorption kinetic process achieved equilibrium within a contact time of 90 min. The sorption isotherm data were simulated by the Langmuir model well and the maximum sorption capacity was calculated to be 203.54 mg/g at 298 K. The Fe_3O_4/CM-CD composite exhibited favorable removal performance toward BB3 in both the single-solute system and the simulation effluent. After sorption equilibrium, the BB3-loaded composite could be easily regenerated and reused for multiple sorption/desorption cycles. The experimental findings herein proposed the feasibility of adopting Fe_3O_4/CM-CD composite for the decontamination of BB3 from the polluted water systems.

Keywords: Fe_3O_4/CM-CD composite; C.I. Basic Blue 3; Simulation effluent; Magnetic separation; Renewable performance

1. Introduction

Basic dyes, for example, C.I. Basic Violet 14, C.I. Basic Orange 2, methylene blue, rhodamine B and C.I. Basic Blue 3 (BB3), are extensively used in the dyeing processes of various textiles such as silk, nylon, acrylon and wool [1,2]. Owing to the presence of aromatic groups and metals in their molecular structures, basic dyes are regarded as one of the most toxic substances [3,4]. The discharge of untreated basic dye-bearing wastewater into the aquatic systems causes severe water pollution and poses serious threat to the health of aquatic organisms. The basic dyes with dark color would greatly decrease the penetration of sunlight and consequently reduce the photosynthetic effectiveness of aquatic plants. In addition, basic dyes and their derivatives even possess mutagenic, teratogenic or carcinogenic impacts on human beings [3–5]. Hence, it is important to develop advanced techniques and cost-effective materials for the decontamination of basic dyes from aqueous solution.

A series of technologies, including coagulation/flocculation [6,7], photocatalysis [8], oxidation [9], membrane filtration [10], sorption [11] and bioremediation [12], have been adopted for the purification of basic dye-bearing wastewaters. Due to their complicated structures, basic dyes are relatively resistant to aerobic digestion, microbial degradation as well as light, heat and oxidizing treatment [4,8–10,12]. These characteristics restrict the potential application of photocatalysis, oxidation,

* Corresponding author.

membrane filtration and bioremediation approaches. The membrane processes bear the defects of low flux and high fouling tendency [10]. In contrast, coagulation/flocculation and sorption are superior to the foregoing water treatment techniques due to their simple design, ease operation, wide suitability, low cost and high efficiency [6,7,11,13]. A variety of adsorbent materials, such as sepiolite, fly ash, apricot shell activated carbon [14], rice hull [15], cation exchange resin (e.g., Lewatit MonoPlus SP 112, Dowex Optipore SD 2 and Amberlite XAD 1180) [16], quartenized sugarcane bagasse [17], organo-modified bentonite [18], poly(amic acid)-treated *Corynebacterium glutamicum* [19], pineapple plant stem [20], Aleppo pine-tree sawdust [21] and graphene oxide [22], have been synthesized for the capture of BB3 and other basic dyes from the solution. However, the further usage of these solid materials is limited since they are difficult to be separated from the liquid phase. Fortunately, this defect can be remedied by integrating the convenient separation property of magnetic nanoparticles and the high complexing ability of polymers for environmental contaminates. Previous studies showed that dyes can be effectively captured by a series of magnetic composites, for example, Fe_3O_4/activated carbon [23], magnetic alginate beads [24], magnetic multi-wall carbon nanotubes [25,26], reduced graphene oxide supported ferrite [27], magnetic chitosan composites [28–30], poly(methylacrylate)-modified Fe_3O_4 composite [31] and Fe_3O_4 supported chitosan–graphene oxide composite [32]. In brief, magnetic adsorbents would exhibit favorable application prospect in the remediation of dye-polluted environment.

In this study, carboxymethyl-β-cyclodextrin (CM-CD) molecules were conjugated with the magnetic Fe_3O_4 nanoparticles by using a co-precipitation method. The properties of the as-prepared Fe_3O_4/CM-CD composite were measured by using a series of characterization approaches such as powder X-ray diffraction (PXRD), zeta potential analysis, magnetization measurements and stability test. BB3, a cationic dye, was selected as the target pollutant due to its wide application in the textile industries [2,13–16,20–22]. Batch technique was then adopted to determine the removal performance of Fe_3O_4/CM-CD toward BB3 as a function of contact time, solution pH, ionic strength, solid dosage and temperature. The sorption kinetics and isotherms were simulated by using the theoretical models to deduce the underlying removal mechanisms. The regeneration and reusability property of Fe_3O_4/CM-CD composite was tested by conducting six cycles of sorption/desorption experiments. According to the experimental results, the feasibility of using Fe_3O_4/CM-CD composite for the disposal of BB3-containing effluent was further evaluated.

2. Experimental details

2.1. Materials and reagents

The reagents $FeCl_2{\cdot}4H_2O$ and $FeCl_3{\cdot}6H_2O$ were purchased from Sinopharm Chemical Reagent Co., Ltd. (China). CM-CD and cationic dye BB3 were obtained from ShangHai YuanYe Biotechnology Co., Ltd. (Pudong County, Shanghai, P.R. China). The stock solution of BB3 (500 mg/L) was prepared by dissolving 0.25 g of BB3 into 500 mL of Milli-Q water. The prepared BB3 stock solution was diluted to obtain the required concentrations in the following experiments.

2.2. Preparation and characterization of magnetic materials

The Fe_3O_4 nanoparticles and Fe_3O_4/CM-CD composite were synthesized by adopting the co-precipitation method as described in the previous literatures [33,34]. Briefly, 5.5 g of $FeCl_3{\cdot}6H_2O$ and 4.0 g of $FeCl_2{\cdot}4H_2O$ were dissolved in 100 mL of Milli-Q water and heated to 80°C. Then, 50 mL of ammonium hydroxide (25%) solution containing 1.0 g of CM-CD was subsequently added into the beaker. The obtained mixture was mechanically agitated under nitrogen condition for 2 h and then cooled to room temperature. The formed Fe_3O_4/CM-CD precipitates were collected with the aid of a magnet. Afterwards, the wet paste was repeatedly washed with ethanol and Milli-Q water and then dried in a vacuum oven. The Fe_3O_4 nanoparticles were prepared via a similar approach without the addition of CM-CD. By using the N_2-BET approach, the specific surface areas of the synthesized Fe_3O_4 nanoparticles and Fe_3O_4/CM-CD composite were measured to be 64.5 and 60.4 m^2/g, respectively. The PXRD patterns were recorded on a Bruker D8 Advance diffractometer from 10° to 70° with a step size of 0.02°. The zeta potentials of the adsorbents as a function of solution pH were measured by using a Zetasizer Nano ZS Analyzer. The magnetism measurements were carried out on a MPMS-XL SQUID magnetometer.

2.3. Sorption experiments

Batch experiments were carried out to determine the sorption behaviors of BB3 on the magnetic materials under different conditions. Specifically, the sorption experiments were performed at a constant solid–liquid ratio of 1.0 g/L except for the effect of solid dosage. The sorption isotherms were measured at three temperatures of 298, 313 and 328 K, while other bath experiments were carried out at 298 K. Briefly, the stock solutions of adsorbent, NaCl electrolyte solution and BB3 were added in a series of amber environmental protection agency vials. The resulting suspensions were adjusted to the desired pH values by adding trace amounts of HCl and/or NaOH solutions. After gently shaken for 24 h, the suspension was exposed to an external magnet to separate the solid from the liquid phase. The obtained supernatant was percolated through a 0.22 μm filtering membrane and the BB3 concentration in the filtrate was measured by visible spectrophotometry at a wavelength of 654 nm. The sorption percentage (sorption% = $(C_0 - C_e)/C_0 \times 100\%$) and sorption amount ($q_e = (C_0 - C_e)\cdot V/m$, mg/g) were then calculated from the initial BB3 concentration (C_0, mg/L), the final BB3 concentration (C_e, mg/L) and the solid-to-liquid ratio (m/V, g/L) of magnetic sorbents.

3. Results and discussion

3.1. Characterization of prepared adsorbents

Fig. 1(A) illustrates the PXRD patterns of the synthesized magnetic materials. The diffraction peaks located at 30.3°, 35.7°, 43.3°, 53.7°, 57.2° and 62.9° represent the (220), (311), (400), (422), (511) and (440) planes of cubic magnetite (Fe_3O_4) phase, respectively [33,35,36]. The PXRD pattern of Fe_3O_4/CM-CD is similar to that of Fe_3O_4 nanoparticles, indicating that the crystalline phase of the magnetite cores is

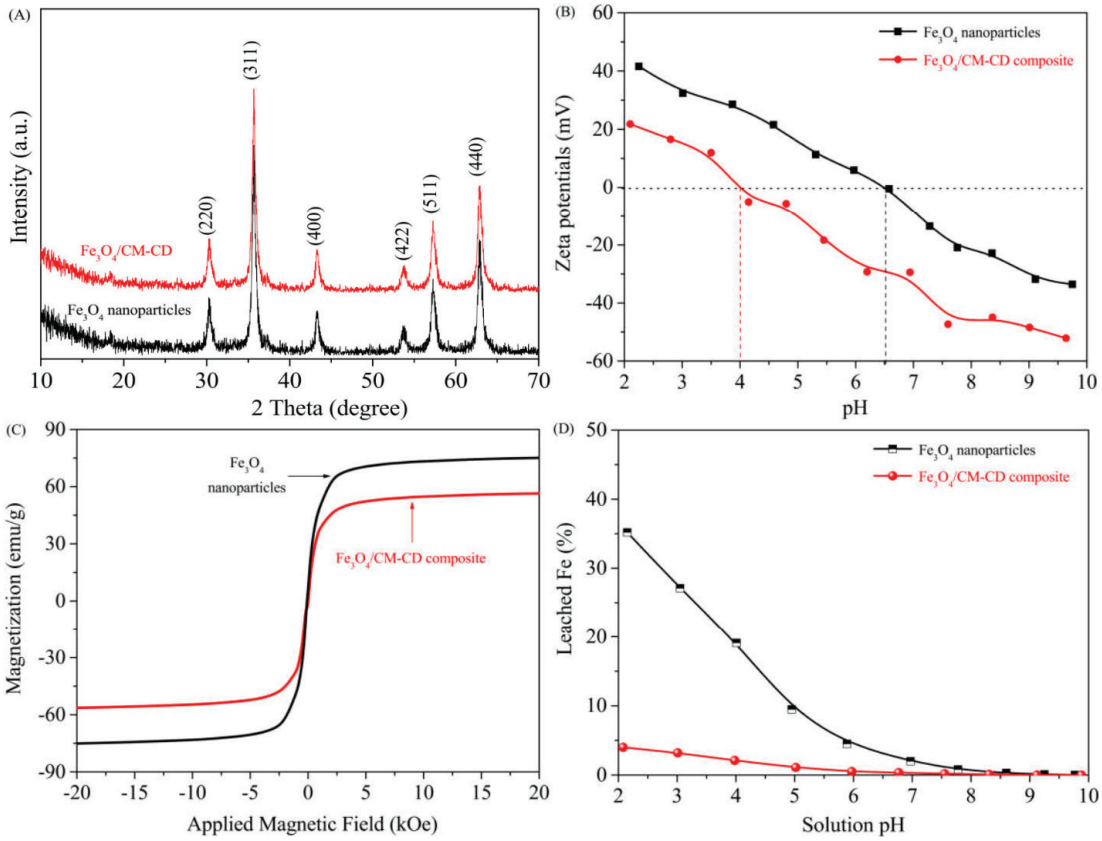

Fig. 1. (A) PXRD patterns of Fe_3O_4 nanoparticles and Fe_3O_4/CM-CD composite. (B) Zeta potentials of Fe_3O_4 nanoparticles and Fe_3O_4/CM-CD composite. T = 298 K, m/V = 1.0 g/L, I = 0.01 mol/L NaCl. (C) Magnetization curves of Fe_3O_4 nanoparticles and Fe_3O_4/CM-CD composite. (D) Relative proportion of Fe leaching from Fe_3O_4 nanoparticles and Fe_3O_4/CM-CD composite in the pH range of 2.0–10.0. T = 298 K, m/V = 1.0 g/L, I = 0.01 mol/L NaCl.

not affected by the surface coating of CM-CD moieties. As shown in Fig. 1(B), the zero point charge (pH_{zpc}) values of Fe_3O_4/CM-CD composite (~4.0) is lower than that of Fe_3O_4 nanoparticles (~6.5). This phenomenon suggests that CM-CD has been successfully introduced on the Fe_3O_4 surfaces. These CM-CD moieties would provide affluent sites (e.g., hydroxyl, –OH; and carboxymethyl, $–CH_2COOH$) and also hydrophobic cavities for the binding of BB3 molecules. According to the magnetic curves (Fig. 1(C)), the Fe_3O_4 nanoparticles and Fe_3O_4/CM-CD composite show the saturation magnetization (M_s) values of ~75.0 and ~56.5 emu/g, respectively. It is clear that the surface coating of CM-CD moieties on the surfaces of Fe_3O_4 leads to the decrease of the M_s value. Nevertheless, the Fe_3O_4/CM-CD composite is still easy to be separated from the aqueous solution with an external magnet. This convenient separation property is conducive to its recovery after sorption equilibrium. The magnetization curves have been previously adopted to quantitatively calculate the weight percentage of polymers grafted on the solid surfaces [34,37–39]. Herein, the difference of 18.5 emu/g indicates a mass fraction of ~24.6% CM-CD in the prepared Fe_3O_4/CM-CD composite. Fig. 1(D) presents the proportion of Fe leaching from the pristine Fe_3O_4 nanoparticles and Fe_3O_4/CM-CD composite in the pH range of 2.0–10.0. For Fe_3O_4, the leaching percentage of Fe greatly decreases from ~35% to zero as the solution pH increases from ~2.0 to ~8.0. While for Fe_3O_4/CM-CD composite, the proportion of leached Fe gradually decreases from ~4% at pH ~2.0 to zero at pH ~6.0. It is clear that the leaching percentage of Fe from Fe_3O_4/CM-CD composite is much lower than that from Fe_3O_4. This result implies that the surface decoration of CM-CD layers effectively prevent the dissolution of inner Fe_3O_4 particles and correspondingly enhances the stability of the synthesized Fe_3O_4/CM-CD composite.

3.2. *Effect of contact time*

Fig. 2 illustrates the time-dependent sorption trends of BB3 on pure Fe_3O_4 and Fe_3O_4/CM-CD composite. The sorption amounts increase rapidly with prolonged contact time and maintain almost constant after 90 min. Note that the short time for separating the adsorbent materials from the aqueous phase by using a magnet is negligible when calculating the total contact time. The fast removal kinetics herein can be attributed to the rapid transport of BB3 from the solution onto the binding sites of the two magnetic adsorbents without obvious diffusion resistance [38–40]. Similar kinetic data were also obtained for the sorption of BB3 onto a series of solid materials such as Aleppo pine-tree sawdust [21], tartaric acid modified sunflower stem [41], sewage treatment plant biosolids [42] and carboxylic group containing cyclodextrin polymer [43]. Equilibrium time is usually regarded as an important factor when evaluating the application potential

of an adsorbent in effluent disposal. In view of the short sorption kinetics, Fe_3O_4/CM-CD composite can be potentially applied in the continuous purification of BB3-polluted water systems. Owing to its high magnetism (Fig. 1(C)), the BB3-loaded adsorbent can be conveniently collected after the sorption equilibrium by using a magnet and regenerated for another sorption/desorption cycle.

As shown in Fig. 2, the sorption amount of BB3 on Fe_3O_4/CM-CD composite (115.60 mg/g) is ~2.0 times higher than that on Fe_3O_4 nanoparticles (58.05 mg/g). As mentioned above, the specific surface area of pristine Fe_3O_4 slightly decreases from 64.5 to 60.4 m^2/g after CM-CD coating. This variation trend indicates that the specific surface area is not the controlling factor for the enhanced sorption amount. Alternatively, the higher sorption property of Fe_3O_4/CM-CD composite toward BB3 is induced by the surface-coated CM-CD moieties. The CM-CD molecule has a truncated-cone structure with abundant hydrophilic hydroxyl and carboxymethyl sites on the external surfaces as well as hydrophobic cavity in the interior [33,44]. As shown in Fig. 1(D), Fe_3O_4/CM-CD exhibits higher stability than Fe_3O_4 nanoparticles over a wide pH range. In addition, the decoration of CM-CD molecules on the surfaces of Fe_3O_4 nanoparticles would greatly reduce their aggregation in solution as reported in previous studies [37,38], which accordingly enhances the dispersion of Fe_3O_4/CM-CD composite. As a result, the surface sites of Fe_3O_4/CM-CD composite would be more available and effective for binding BB3. Herein, the sorption kinetic experiment is carried out at a pH value of 5.0, which is lower than the pH_{zpc} value of Fe_3O_4 nanoparticles (i.e., ~6.5), while higher than that of Fe_3O_4/CM-CD (i.e., ~4.0; Fig. 1(B)). The surfaces of Fe_3O_4 nanoparticles are positively charged due to the protonation reaction, while the Fe_3O_4/CM-CD surfaces are negatively charged due to the deprotonation reaction. Under such circumstances, the BB3 molecules with positive charge would be preferentially attached to the surfaces of Fe_3O_4/CM-CD due to electrostatic attraction. With the increase of contact time, the surface-bound BB3 molecules would gradually enter the internal cylindrical cavity of CM-CD moieties due to hydrophobic interaction, resulting in the formation of stable inclusion complexes.

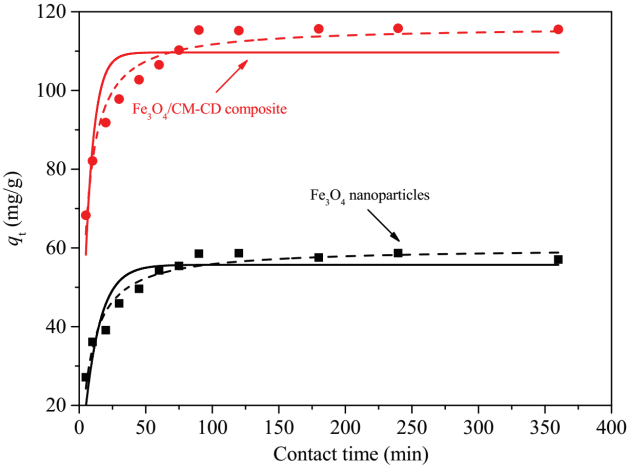

Fig. 2. Sorption kinetics data of BB3 on magnetic adsorbents and the fit curves by using pseudo-first-order and pseudo-second-order models. T = 298 K, pH = 5.0, m/V = 1.0 g/L, C_{BB3} = 150 mg/L, I = 0.01 mol/L NaCl. Symbols represent the experimental data, solid lines represent the fit curves of pseudo-first-order model and dash lines represent the fit curves of pseudo-second-order model.

Several mechanisms may be involved in the sorption kinetic processes of dyes on solid materials, including physical sorption, hydrogen bonding, diffusion and chemisorption. In order to deduce the removal mechanisms of BB3 by the magnetic materials, the pseudo-first-order and pseudo-second-order kinetics models were adopted to simulate the sorption kinetics data. Specifically, the pseudo-first-order model (Eq. (1)) is based on the assumption that the sorption procedure is dominated by diffusion, while the pseudo-second-order model (Eq. (2)) is based on the assumption that the sorption process is driven by chemisorption involving electron sharing/transfer and/or surface complexation between pollutants and solid materials [45–49].

$$q_t = q_{e,\mathrm{cal}}(1 - e^{-k_1 t}) \tag{1}$$

$$q_t = q_{e,\mathrm{cal}} \frac{k_2 t}{1 + k_2 t} \tag{2}$$

In the equations, k_1 (min^{-1}) and k_2 (g/mg·min) are the rate constants of pseudo-first-order and pseudo-second-order models, respectively; $q_{e,\mathrm{cal}}$ is the theoretical sorption amount (mg/g) under equilibrium condition. One can see from the fit results in Fig. 2 as well as the correlation coefficient (R^2) values in Table 1 that the sorption kinetic data of BB3 are better simulated by the pseudo-second-order model. In addition, the $q_{e,\mathrm{cal}}$ values obtained from the model fits are comparable with the $q_{e,\mathrm{exp}}$ values. This result suggests that chemisorption rather than diffusion is the predominant driving force for the removal of BB3 by the magnetic materials. In a series of previous studies [50–53], the sorption kinetics of BB3 and other basic dyes onto various solid materials was also reported to be well fitted by the pseudo-second-order model. However, the sorption kinetic data of BB3 on the wood activated charcoal followed the pseudo-second-order model, indicating that physical sorption was the main removal mechanism [54]. The differences observed in the foregoing literatures can be

Table 1
The kinetic parameters of BB3 sorption on pure Fe_3O_4 and Fe_3O_4/CM-CD composite

Kinetics models	Parameters	Pure Fe_3O_4	Fe_3O_4/CM-CD
Pseudo-first-order	k_1 (min^{-1})	0.086	0.152
	$q_{e,\mathrm{exp}}$ (mg/g)	58.05	115.60
	$q_{e,\mathrm{cal}}$ (mg/g)	55.72	109.66
	R^2	0.815	0.746
Pseudo-second-order	k_2 (g/min mg)	0.136	0.240
	$q_{e,\mathrm{exp}}$ (mg/g)	58.05	115.60
	$q_{e,\mathrm{cal}}$ (mg/g)	60.02	116.34
	R^2	0.946	0.953

attributed to the diversities in the physicochemical properties of the applied adsorbents.

3.3. Effect of pH and ionic strength

Fig. 3 shows the pH-dependent sorption behaviors of BB3 on Fe_3O_4/CM-CD composite in 0.001, 0.01 and 0.1 mol/L of NaCl electrolyte solutions, respectively. It is clear that solution pH plays a significant role in BB3 sorption procedure. Specifically in 0.01 mol/L of NaCl solution, the sorption percentage of BB3 increases slowly from ~10% to ~20% as the solution pH rises from 2.0 to 4.0, then increases sharply to ~98% at pH 7.0, and finally maintains constant at higher pH values. The occurrence of multiple sorption edges suggests the presence of different sequestration mechanisms. As illustrated in Fig. 1(B), the Fe_3O_4/CM-CD composite has a pH_{zpc} value of ~4.0. Its surfaces would be positively charged at pH < 4.0 due to the protonation reaction of the binding sites. Meanwhile, the *N*-ethyl groups of the BB3 molecules would also be protonated at acidic pH (see the illustration in Fig. 3). It is difficult for the binding of positively charged BB3 species on the positively charged surfaces of Fe_3O_4/CM-CD due to electrostatic repulsion. The hydrophilic BB3 molecules at low pH may weakly interact with the hydrophobic cavity of surface-linked CM-CD moieties, leading to a low sorption percentage [33,55]. At pH > 4.0, the electrostatic attraction between positively charged BB3 molecules and negatively charged Fe_3O_4/CM-CD facilitates their binding on the deprotonated surfaces sites. In addition, the BB3 molecules can be easily inserted into the cylindrical cavity of the CM-CD moieties, leading to the sharp increase of BB3 sorption percentage.

As shown in Fig. 3, the rise of ionic strength results in an increase of BB3 sorption percentage at pH < 7.0, while no effect of ionic strength can be observed at pH > 7.0 as nearly all the BB3 molecules are removed from the aqueous solution. Herein, the influence of ionic strength at pH < 7.0 can be tentatively interpreted from the aspects of electrostatic interaction and hydrophobic effect between BB3 and Fe_3O_4/CM-CD composite. Specifically in the pH range of 2.0–4.0 (pH_{zpc} value of the adsorbent), the repulsive electrostatic

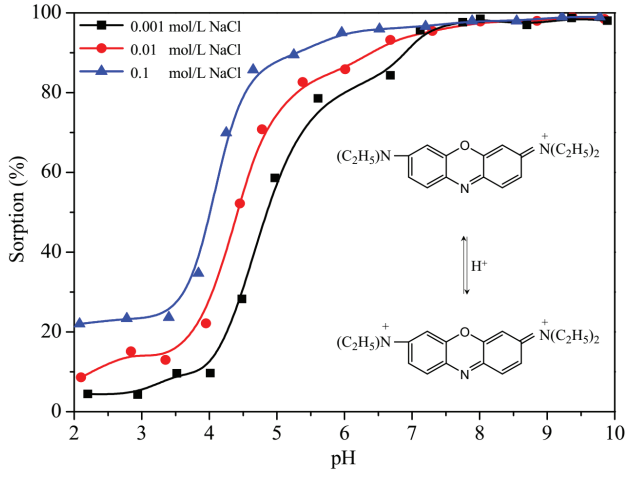

Fig. 3. Sorption of BB3 on Fe_3O_4/CM-CD composite as a function of pH and ionic strength. T = 298 K, C_{BB3} = 150 mg/L, m/V = 1.0 g/L.

interaction occurs between Fe_3O_4/CM-CD composite and BB3 molecules with positive charge. The increase of ionic strength can compress the diffuse electric double layer surrounding the Fe_3O_4/CM-CD surfaces due to the screening effect, which would correspondingly suppress the electrostatic repulsion between the two positively charged components [56–59]. In addition, the rise in ionic strength would also enhance the hydrophobic attraction between BB3 and the cavity of CM-CD moieties [60,61]. As a result, more BB3 molecules are expected to be adsorbed at higher ionic strength. In the pH range of 4.0–7.0, the attractive electrostatic interaction occurs between positively charged BB3 molecules and negatively charged Fe_3O_4/CM-CD surfaces. Under such circumstances, the charge screening effect of electrolyte ions would reduce the sorption affinity of Fe_3O_4/CM-CD toward BB3 and consequently decrease the sorption percentage of BB3 [56,57]. However, our experimental result shows that the increase of NaCl concentration leads to the improvement of BB3 sorption percentage. In view of this, the electrostatic interaction is not the predominant sorption mechanism for the sorption of BB3 on Fe_3O_4/CM-CD. Alternatively, the BB3 molecules are more possibly preferentially adsorbed due to the hydrophobic attraction, leading to the formation of inclusion complexes. This inclusion reaction is enhanced at higher ionic strength and therefore a higher sorption percentage is expected. In addition, the increase of NaCl concentration can enhance the dipole–dipole, ion–dipole and van der Waals forces between BB3 molecules. This variation trend would cause the aggregation and dimerization of BB3 in solution [56,57], which partly contributes to the higher sorption percentage of BB3 at higher ionic strength.

3.4. Effect of solid dosage

The price–performance ratio of adsorbent materials in practical effluent disposal is greatly dependent on the solid dosage required for a favorable removal performance. Herein, the sorption of BB3 on Fe_3O_4/CM-CD at a series of solid-to-liquid ratios (i.e., 0.1–2.0 g/L) was investigated and the results are shown in Fig. 4. As the solid content rises from 0.1 to 1.6 g/L, the sorption percentage gradually increases from ~32% to ~88% (Fig. 4(A)). No obvious change of the sorption percentage can be observed at solid dosage above 1.6 g/L. This result suggests that the sorption percentage of BB3 would not limitlessly increase with increasing Fe_3O_4/CM-CD dosage. For the purpose of reducing the sewage treatment cost, the optimum Fe_3O_4@CMC dosage of 1.6 g/L can be selected for the efficient removal of 150 mg/L of BB3 at a solution pH of 5.0.

As shown in Fig. 4(B), the sorption amount of BB3 shows a decreasing trend with increasing Fe_3O_4/CM-CD content. At lower solid dosage, the adsorbent particles can disperse well in the solution and more active sites are available for the capture of BB3. However, the supersaturation of the suspension at higher solid content would increase the probability for the collision and aggregation of Fe_3O_4/CM-CD particles. This phenomenon would correspondingly result in the reduced availability of the surface sites and the decrease of BB3 sorption amount. Besides, the aggregation of Fe_3O_4/CM-CD particles would prolong the diffusional path of BB3 from the solution to the surfaces and also decrease

the total surface area for the retention of BB3 [62]. Moreover, the collision between Fe_3O_4/CM-CD particles at higher solid dosage may desorb some of the sequestrated BB3 molecules from the adsorbent surfaces and thereby cause the decrease of BB3 sorption amount.

3.5. Effect of temperature

Fig. 5 illustrates the sorption isotherms of BB3 on Fe_3O_4/CM-CD composite at 298, 313 and 328 K, respectively. One can see that the sorption amount of BB3 increases with the rise of its equilibrium concentration in solution. Herein, higher BB3 concentration can promote its contact and interaction with Fe_3O_4/CM-CD composite, which leads to the achievement of a higher sorption amount. The sorption isotherms reveal the typical L shape, indicating that there is no strong competition between the solvent (herein, H_2O) and BB3 molecules to occupy the binding sites of Fe_3O_4/CM-CD composite. Specifically, the rise of temperature is unfavorable for BB3 sorption and leads to the decrease of sorption amount.

In order to further analyze the temperate-dependent sorption behaviors of BB3 on Fe_3O_4/CM-CD composite, the Langmuir (Eq. (3)) and Freundlich (Eq. (4)) models were used to simulate the sorption isotherm data.

$$q_e = \frac{bq_{\max}C_e}{1+bC_e} \tag{3}$$

$$q_e = K_F C_e^{\,n} \tag{4}$$

Herein, C_e (mg/L) is the concentration of BB3 remained in solution after sorption equilibrium; q_e (mg/g) is the equilibrium sorption amount of BB3 on per weight unit of Fe_3O_4/CM-CD; $q_{\max}$ (mg/g) is the maximum sorption capacity of Fe_3O_4/CM-CD toward BB3 at a monolayer coverage; b (L/mg) is a parameter that relates to the sorption heat; K_F (mg^{1-n}·L^n/g) represents the sorption affinity of Fe_3O_4/CM-CD toward BB3, and the value of n is indicative of the specific sorption mode (i.e., linear at $n = 1$ or nonlinear at $n < 1$).

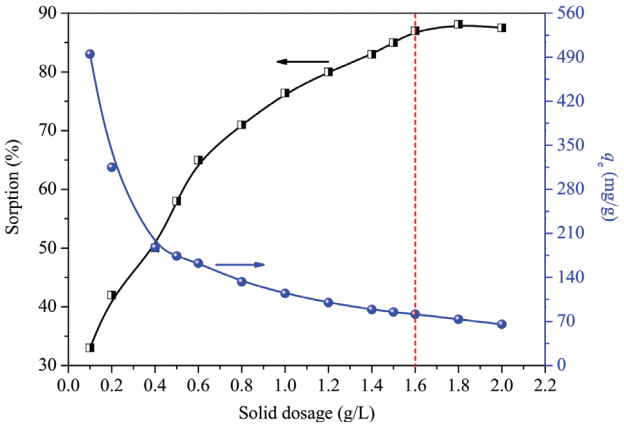

Fig. 4. Sorption percentage and sorption amount of BB3 on Fe_3O_4/CM-CD composite as a function of solid dosage. $T = 298$ K, pH = 5.0, $C_{BB3} = 150$ mg/L, $I = 0.01$ mol/L NaCl.

From the data fit as illustrated in Fig. 5 and the corresponding correlation coefficient (R^2) values as listed in Table 2, one can see that the sorption isotherms are better simulated by the Langmuir model than the Freundlich model. This result indicates that the immobilization of BB3 on Fe_3O_4/CM-CD composite is due to a chemisorption mechanism [63]. It is worth noting that the sorption equilibrium experiments were conducted at different BB3 concentrations by keeping a fixed Fe_3O_4/CM-CD dosage of 1.0 g/L. Under such circumstances, a limited amount of active sites would be provided by the adsorbent for capturing BB3, which correspondingly results in the presence of a saturated sorption amount at higher BB3 concentration. Hence, the sorption isotherms would not be well simulated by the Freundlich model with the assumption that the sorption amount of BB3 is expected to exponentially increase with the increase of its equilibrium concentration in solution. For all the temperatures, the values of $q_{e,\exp}$ are smaller than those of $q_{\max}$ calculated from the Langmuir model simulation. This phenomenon means that the active sites of Fe_3O_4/CM-CD are not completely occupied and the adsorbed BB3 molecules do not interact with each other. The values of n are calculated to be in the range of 0–1, suggesting that the sorption of BB3 on Fe_3O_4/CM-CD composite is a nonlinear and favorable process.

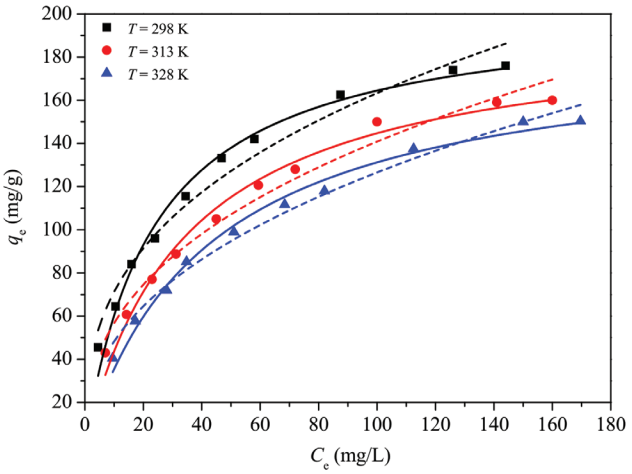

Fig. 5. Sorption isotherms, Langmuir and Freundlich model fits of BB3 on Fe_3O_4/CM-CD composite. pH = 5.0, $m/V = 1.0$ g/L, $I = 0.01$ mol/L NaCl. Symbols represent the sorption isotherm data, solid lines denote the fit curves of Langmuir model and dashed lines denote the fit curves of Freundlich model.

Table 2
Parameters for Langmuir and Freundlich models at different temperatures

Correlation parameters		$T = 298$ K	$T = 313$ K	$T = 328$ K
Langmuir	$q_{\max}$ (mg/g)	203.54	194.82	187.28
	b (L/mg)	0.042	0.029	0.023
	R^2	0.989	0.984	0.986
Freundlich	K_F (mg^{1-n}·L^n/g)	31.06	22.84	18.43
	n	0.360	0.395	0.418
	R^2	0.950	0.948	0.954

The intrinsic thermodynamic parameters of the sorption systems, that is, the changes of Gibbs free energy ($\Delta G°$), enthalpy ($\Delta H°$) and entropy ($\Delta S°$), were further calculated according to the following Eqs. (5)–(7), separately.

$$\Delta G^0 = -RT\ln K^0 \tag{5}$$

$$\Delta S^0 = -\left(\frac{\partial \Delta G^0}{\partial T}\right)_P \tag{6}$$

$$\Delta H^0 = \Delta G^0 + T\Delta S^0 \tag{7}$$

The negative $\Delta G°$ values (Table 3) imply the feasibility and spontaneity of BB3 binding on Fe_3O_4/CM-CD composite without the input of additional energy from outside of the sorption system. Specifically, the value of $\Delta G°$ becomes less negative with the increase of temperature, which results in the decrease of sorption spontaneity and sorption trend. The negative $\Delta S°$ value (Table 3) reveals the occurrence of some structural changes and the reduction of randomness during the sorption process. In other words, the adsorbed BB3 molecules have smaller randomness than those in the bulk solution. The negative $\Delta H°$ values (Table 3) indicate that the removal of BB3 by Fe_3O_4/CM-CD is an exothermic process. A series of previous studies proposed that the interaction affinity of dyes with solvent molecules became stronger than that with adsorbent surfaces at higher temperature [64–66]. Consequently, the dyes would be more difficult to be captured by the adsorbent materials. In addition, the mobility of BB3 molecules would increase with the rise of temperature, which enhances the magnitude of BB3 desorption from the Fe_3O_4/CM-CD surfaces [64]. The increased mobility of dye molecules at the elevated temperatures was also demonstrated by the decreased values of b and K_F as well as the increased values of n as listed in Table 2. The absolute values of $\Delta H°$ are found to be higher than those of $T\Delta S°$ (Table 3), indicating the sorption of BB3 on Fe_3O_4/CM-CD composite is an enthalpy-controlling process rather than an entropy-controlling procedure.

Table 3
Thermodynamic parameters for BB3 sorption on Fe_3O_4/CM-CD composite

T (K)	$\Delta G°$ (kJ/mol)	$\Delta S°$ (J/mol·K)	$T\Delta S°$ (kJ/mol)	$\Delta H°$ (kJ/mol)
298	–7.12		–17.79	–24.91
313	–6.06	–59.70	–18.69	–24.74
328	–5.33		–19.58	–24.93

3.6. Comparison with other adsorbents

To help evaluate the application feasibility of Fe_3O_4/CM-CD in practical effluent disposal, the maximum sorption capacity (i.e., q_{max} derived from Langmuir model fit) of this material toward BB3 is carefully compared with those of other previously reported adsorbents. As listed in Table 4, the q_{max} value of BB3 on Fe_3O_4/CM-CD is higher than those on rice hull [15], *Corynebacterium glutamicum* [19], acrylic resin [13], amberlite XAD 1180 [16], sugarcane bagasse [17], Aleppo pine-tree sawdust [21], fly ash [14], sepiolite [14] and apricot stone activated carbon (ASAC) [14], while lower than those on Dowex Optipore SD 2 and Lewatit MonoPlus SP 112 [16]. The comparison herein indicates that Fe_3O_4/CM-CD exhibits favorable removal performance toward BB3.

3.7. Removal efficiency for simulation wastewater

Considering the heterogeneity and complexity of the real aquatic environment, the removal performance of Fe_3O_4/CM-CD toward BB3 in a simulation wastewater was tested to verify the research findings derived from the single-solute experiments. Specifically, the simulated effluent was composed of 20 mg/L of Cd(II), 20 mg/L of Pb(II), 10 mg/L of As(V), 10 mg/L of Cr(VI), 50 mg/L of 1-naphthol, 150 mg/L of BB3, 20 mg/L of humic acid (to simulate the natural organic matter in the water environment) and 0.01 mol/L of NaCl as the background electrolyte. Herein, the addition of heavy metal ions, anionic and organic pollutants was

Table 4
Comparison of BB3 sorption capacity of Fe_3O_4/CM-CD with other adsorbent materials

Materials	Experimental conditions	q_{max} (mg/g)	References
Rice hull	T = 298 K	13.41	[15]
Corynebacterium glutamicum	pH = 6.0, T = 298 K	27.95	[19]
Acrylic resin	pH = 5.5, T = 290 K	34.36	[13]
Amberlite XAD 1180	pH = 4.3, T = 293 K	35.70	[16]
Sugarcane bagasse	pH = 6.0, T = 293 K	37.59	[17]
Aleppo pine-tree sawdust	T = 293 K	65.36	[21]
Fly ash	T = 303 K	128.21	[14]
Sepiolite	T = 303 K	155.52	[14]
ASAC	T = 303 K	181.50	[14]
Fe_3O_4/CM-CD	pH = 5.0, T = 298 K	203.54	This study
Dowex Optipore SD 2	pH = 4.3, T = 293 K	270.90	[16]
Lewatit MonoPlus SP 112	pH = 4.3, T = 293 K	560.70	[16]

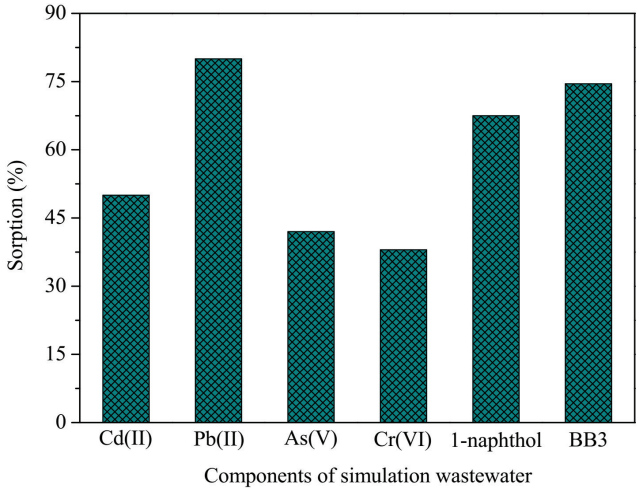

Fig. 6. Removal performance of Fe_3O_4/CM-CD toward BB3 in the simulation wastewater.

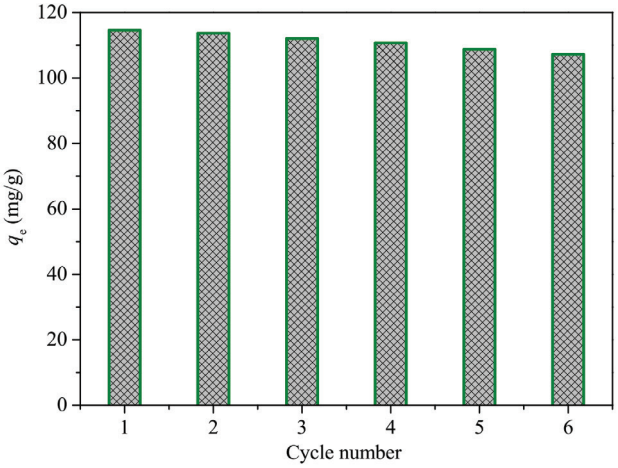

Fig. 7. Regeneration and reusability of Fe_3O_4/CM-CD composite in the removal of BB3. T = 298 K, pH = 5.0, m/V = 1.0 g/L, C_{BB3} = 150 mg/L, I = 0.01 mol/L NaCl.

due to their extensive distribution in the mixed wastewater discharged by a series of industrial processes, for example, galvanization, machinery, electronics, catalysis, batteries manufacturing, pigment processing, petroleum refining, medical diagnosis, pesticide production, chemical engineering, etc. Typical experiment was conducted by adding 150 mL of the simulation wastewater into a 500 mL beaker. The subsequent removal test was carried out at pH 5.0 by using a similar method as that for batch experiments. As shown in Fig. 6, a 1.0 g/L of Fe_3O_4/CM-CD results in the removal of ~51% Cd(II), ~80% Pb(II), ~42% As(V), ~38% Cr(VI), ~67% 1-naphthol and ~74% BB3. Herein, the co-sorption behavior of multiple components on Fe_3O_4/CM-CD is possibly controlled by various driving forces such as electrostatic interaction, surface complexation, ligand exchange, hydrophobic action and inclusion effect [19,33,44,56–61]. Specifically, the removal percentage of BB3 from the simulation wastewater (~74%) is comparable to that from the single-solute system (~77% at pH 5.0 as illustrated in Fig. 3), indicating the ignorable influence of coexisting chemical constituents on the decontamination of BB3. It is undeniable that the compositions in the simulation wastewater are somewhat different from those in the real effluent. Nevertheless, the result herein demonstrates the feasibility of using Fe_3O_4/CM-CD composite for the purification of actual BB3-containing wastewater.

3.8. Regeneration and reusability property

The regeneration and recyclability of Fe_3O_4/CM-CD composite was explored to evaluate its application potential in the purification of BB3-polluted wastewater. It was reported that almost 100% of the sequestrated methylene blue could be desorbed from the CM-CD conjugated magnetic nanoadsorbent by using a methanol solution containing acetic acid (5% (v/v)) as eluent [33]. Considering the similarity between the molecular structure of BB3 and methylene blue, the same strippant was used in the present study to conduct the desorption experiments and the regenerated Fe_3O_4/CM-CD composites were then used for six successive rounds. As illustrated in Fig. 7, the sorption amount of BB3 slightly decreases from ~115 to ~108 mg/g after six rounds of adsorption/desorption tests. The small decline of BB3 sorption amount may be due to the slight loss of Fe_3O_4/CM-CD dosage during the recovery process. Nevertheless, the experimental result herein shows that Fe_3O_4/CM-CD composite exhibits favorable regeneration capacity and excellent reusability performance for the removal of BB3. In other words, this material can guarantee long-term application in the disposal of BB3-polluted water.

Herein, the cost of Fe_3O_4/CM-CD is evaluated to further determine its application potential in the practical wastewater treatment. Specifically, this magnetic composite can be rapidly and simply synthesized by using the co-precipitation method. The raw materials, that is, $FeCl_3{\cdot}6H_2O$, $FeCl_2{\cdot}4H_2O$ and CM-CD, have relatively low prices of ca. US$5.8/500g, US$7.3/500g and US$218.1/500g, respectively. Hence, the cost for preparing Fe_3O_4/CM-CD composite is calculated to be ca. US$0.2/g on the basis of the synthesis procedure. By integrating the low production cost with the satisfactory recycling ability as verified above, one can conclude that Fe_3O_4/CM-CD would be an economical and applicable adsorbent for the treatment of BB3-bearing wastewater.

4. Conclusions

The present work reported the synthesis of magnetic Fe_3O_4/CM-CD composite for the removal of BB3 from the aqueous solution. The usage of nontoxic raw materials (iron salts and CM-CD) and the application of simple chemical co-precipitation approach ensured the safety and cheapness of the adsorbent material. The surface-coated CM-CD moieties improved the stability of Fe_3O_4/CM-CD in solution. Batch experiments were carried out to investigate the removal performance of Fe_3O_4/CM-CD toward BB3 as a function of contact time, solution pH, ionic strength, solid dosage and temperature. The sorption kinetic data were well simulated by the pseudo-second-order equation, suggesting chemisorption was the underlying sequestration mechanism of BB3 by Fe_3O_4/CM-CD composite. The calculated thermodynamic parameters pointed to the occurrence of an exothermic, spontaneous and entropy decreasing sorption process.

The sorption/desorption experiments suggested that Fe_3O_4/CM-CD composite possessed favorable regeneration capacity and excellent reusability performance for the removal of BB3. Owing to its low production cost, environmental friendliness, high stability, high sorption capacity, favorable recyclability and convenient separation property, Fe_3O_4/CM-CD composite could be potentially used as a good adsorbent for the purification of BB3-bearing effluents.

Acknowledgment

Financial supports from the Science and Technology Project of Shaoxing (2014B70041) are acknowledged.

Conflict of interest

The authors confirm that this article has no conflict of interest.

References

[1] G. Crini, P. Badot, Application of chitosan, a natural aminopolysaccharide, for dye removal from aqueous solutions by adsorption processes using batch studies: a review of recent literature, Prog. Polym. Sci., 33 (2008) 399–447.
[2] M. Shahid, Shahid-ul-Islam, F. Mohammad, Recent advancements in natural dye applications: a review, J. Cleaner Prod., 53 (2013) 310–331.
[3] US EPA, Best Management Practice for Pollution Prevention in the Textile Industry, EPA/625/R-96/004, Ohio, 1996.
[4] K. Marungruenga, P. Pavasant, Removal of basic dye (Astrazon Blue FGRL) using macroalga *Caulerpa lentillifera*, J. Environ. Manage., 78 (2006) 268–274.
[5] S. Hosseini, M.A. Khan, M.R. Malekbala, W. Cheah, T.S.Y. Choong, Carbon coated monolith, a mesoporous material for the removal of methyl orange from aqueous phase: adsorption and desorption studies, Chem. Eng. J., 171 (2011) 1124–1131.
[6] C.S. Lee, J. Robinson, M.F. Chong, A review on application of flocculants in wastewater treatment, Process Saf. Environ., 92 (2014) 489–508.
[7] R. Yang, H.J. Li, M. Huang, H. Yang, A.M. Li, A review on chitosan-based flocculants and their applications in water treatment, Water Res., 95 (2016) 59–89.
[8] A.R. Khataee, M. Fathinia, S. Aber, Kinetic study of photocatalytic decolorization of C.I. Basic Blue 3 solution on immobilized titanium dioxide nanoparticles, Chem. Eng. Res. Des., 89 (2011) 2110–2116.
[9] M.A. Oturan, J.J. Aaron, Advanced oxidation processes in water/wastewater treatment: principles and applications. A review, Crit. Rev. Environ. Sci. Technol., 44 (2014) 2577–2641.
[10] P. Chegoonian, M. Feiz, S.A. Hosseini Ravandi, S. Mallakpour, Preparation of sulfonated poly(ethylene terephthalate) submicron fibrous membranes for removal of basic dyes, J. Appl. Polym. Sci., 24 (2012) E190–E198.
[11] M.T. Yagub, T.K. Sen, S. Afroze, H.M. Ang, Dye and its removal from aqueous solution by adsorption: a review, Adv. Colloid Interface Sci., 209 (2014) 172–184.
[12] P. Ramachandran, R. Sundharam, J. Palaniyappan, A.P. Munusamy, Potential process implicated in bioremediation of textile effluents: a review, Adv. Appl. Sci. Res., 4 (2013) 131–145.
[13] A. Bârsănescu, R. Buhăceanu, V. Dulman, Removal of Basic Blue 3 by sorption onto a weak acid acrylic resin, J. Appl. Polym. Sci., 113 (2009) 607–614.
[14] B. Karagozoglu, M. Tasdemir, E. Demirbas, M. Kobya, The adsorption of basic dye (Astrazon Blue FGRL) from aqueous solutions onto sepiolite, fly ash and apricot shell activated carbon: kinetic and equilibrium studies, J. Hazard. Mater., 147 (2007) 297–306.
[15] S.T. Ong, C.K. Lee, Z. Zainal, Removal of basic and reactive dyes using ethylenediamine modified rice hull, Bioresour. Technol., 98 (2007) 2792–2799.
[16] M. Wawrzkiewicz, Removal of C.I. Basic Blue 3 dye by sorption onto cation exchange resin, functionalized and non-functionalized polymeric sorbents from aqueous solutions and wastewaters, Chem. Eng. J., 217 (2013) 414–425.
[17] S.Y. Wong, Y.P. Tan, A.H. Abdullah, S.T. Ong, The removal of basic and reactive dyes using quartenised sugar cane bagasse, J. Phys. Sci., 20 (2009) 59–74.
[18] S. Hashemian, B. Sadeghi, F. Mozafari, H. Salehifar, K. Salari, Adsorption of disperse of yellow 42 onto bentonite and organo-modified bentonite by tetra butyl ammonium iodide (B-TBAI), Pol. J. Environ. Stud., 22 (2013) 1363–1370.
[19] S.W. Won, K. Vijayaraghavan, J. Mao, S. Kim, Y.S. Yun, Reinforcement of carboxyl groups in the surface of *Corynebacterium glutamicum* biomass for effective removal of basic dyes, Bioresour. Technol., 100 (2009) 6301–6306.
[20] S.L. Chan, Y.P. Tan, A.H. Abdullah, S.T. Ong, Equilibrium, kinetic and thermodynamic studies of a new potential biosorbent for the removal of basic blue 3 and congo red dyes: pineapple (*Ananas comosus*) plant stem, J. Taiwan Inst. Chem. Eng., 61 (2016) 306–315.
[21] N. Ouazene, A. Lounis, Adsorption characteristics of CI Basic Blue 3 from aqueous solution onto Aleppo pine-tree sawdust, Color. Technol., 128 (2011) 21–27.
[22] H. Yan, X. Tao, Z. Yang, K. Li, H. Yang, A.M. Li, R.S. Cheng, Effects of the oxidation degree of graphene oxide on the adsorption of methylene blue, J. Hazard. Mater., 268 (2014) 191–198.
[23] N. Yang, S. Zhu, D. Zhang, S. Xu, Synthesis and properties of magnetic Fe_3O_4-activated carbon nanocomposite particles for dye removal, Mater. Lett., 62 (2008) 645–647.
[24] V. Rocher, J.M. Siaugue, V. Cabuil, A. Bee, Removal of organic dyes by magnetic alginate beads, Water Res., 42 (2008) 1290–1298.
[25] J.L. Gong, B. Wang, G.M. Zeng, C.P. Yang, C.G. Niu, Q.Y. Niu, W.J. Zhou, Y. Liang, Removal of cationic dyes from aqueous solution using magnetic multi-wall carbon nanotube nanocomposite as adsorbent, J. Hazard. Mater., 164 (2009) 1517–1522.
[26] Ş.S. Bayazit, Magnetic multi-wall carbon nanotubes for methyl orange removal from aqueous solutions: equilibrium, kinetic and thermodynamic studies, Sep. Sci. Technol., 49 (2014) 1389–1400.
[27] S. Bai, X.P. Shen, X. Zhong, Y. Liu, G.X. Zhu, X. Xu, K.M. Chen, One-pot solvothermal preparation of magnetic reduced graphene oxide-ferrite hybrids for organic dye removal, Carbon, 50 (2012) 2337–2346.
[28] A. Debrassi, T. Baccarin, C. Albertina Demarchi, N. Nedelko, A. Ślawska-Waniewska, P. Dłużewski, M. Bilska, C.A. Rodrigues, Adsorption of Remazol Red 198 onto magnetic *N*-lauryl chitosan particles: equilibrium, kinetics, reuse and factorial design, Environ. Sci. Pollut. Res., 19 (2012) 1594–1604.
[29] D.H.K. Reddy, S.M. Lee, Application of magnetic chitosan composites for the removal of toxic metal and dyes from aqueous solutions, Adv. Colloid Interface Sci., 201–202 (2013) 68–93.
[30] K. Li, P. Li, J. Cai, S.J. Xiao, H. Yang, Efficient adsorption of both methyl orange and chromium from their aqueous mixtures using a quaternary ammonium salt modified chitosan magnetic composite adsorbent, Chemosphere, 154 (2016) 310–318.
[31] A. Pourjavadi, A. Abedinmoghanaki, S.A. Nasseri, A new functionalized magnetic nanocomposite of poly(methylacrylate) for the efficient removal of anionic dyes from aqueous media, RSC Adv., 6 (2016) 7982–7989.
[32] K. Gula, S. Sohni, M. Waqar, F. Ahmad, N.A. Nik Norulaini, A.K.M. Omar, Functionalization of magnetic chitosan with graphene oxide for removal of cationic and anionic dyes from aqueous solution, Carbohydr. Polym., 152 (2016) 520–531.
[33] A.Z.M. Badruddoza, G.S.S. Hazel, K. Hidajat, M.S. Uddin, Synthesis of carboxymethyl-β-cyclodextrin conjugated magnetic nano-adsorbent for removal of methylene blue, Colloids Surf., A, 367 (2010) 85–95.

[34] P.F. Tang, J. Shen, Z.D. Hu, G.L. Bai, M. Wang, B.J. Peng, R.P. Shen, W.S. Linghu, High-efficient scavenging of U(VI) by magnetic Fe_3O_4@gelatin composite, J. Mol. Liq., 221 (2016) 497–506.
[35] M.H. Liao, D.H. Chen, Preparation and characterization of a novel magnetic nano-adsorbent, J. Mater. Chem., 12 (2002) 3654–3659.
[36] Y.C. Chang, D.H. Chen, Preparation and adsorption properties of monodisperse chitosan-bound Fe_3O_4 magnetic nanoparticles for removal of Cu(II) ions, J. Colloid Interface Sci., 283 (2005) 446–451.
[37] J.F. Liu, Z.S. Zhao, G.B. Jiang, Coating Fe_3O_4 magnetic nanoparticles with humic acid for high efficient removal of heavy metals in water, Environ. Sci. Technol., 42 (2008) 6949–6954.
[38] S.T. Yang, P.F. Zong, X.M. Ren, Q. Wang, X.K. Wang, Rapid and highly efficient preconcentration of Eu(III) by core-shell structured Fe_3O_4@humic acid magnetic nanoparticles, ACS Appl. Mater. Interfaces, 4 (2012) 6891–6900.
[39] X.B. Zhang, Y. Wang, S.T. Yang, Simultaneous removal of Co(II) and 1-naphthol by core-shell structured Fe_3O_4@cyclodextrin magnetic nanoparticles, Carbohydr. Polym., 114 (2014) 521–529.
[40] S.X. Zhang, H.Y. Niu, Y.Q. Cai, X.L. Zhao, Y.L. Shi, Arsenite and arsenate adsorption on coprecipitated bimetal oxide magnetic nanomaterials: $MnFe_2O_4$ and $CoFe_2O_4$, Chem. Eng. J., 158 (2010) 599–607.
[41] S.M. Ghasemi, H.A. Asgharnia, K. Karimyan, S. Adabi, Adsorption of Basic Blue3 (BB3) dye from aqueous solution by tartaric acid modified sunflower stem: kinetics and equilibrium studies, Int. Res. J. Appl. Basic Sci., 9 (2015) 686–694.
[42] M.Z. Alam, Biosorption of basic dyes using sewage treatment plant biosolids, Biotechnology, 3 (2004) 1149–1156.
[43] G. Crini, Kinetic and equilibrium studies on the removal of cationic dyes from aqueous solution by adsorption onto a cyclodextrin polymer, Dyes Pigm., 77 (2008) 415–426.
[44] A.Z.M. Badruddoza, A.S.H. Tay, P.Y. Tan, K. Hidajat, M.S. Uddin, Carboxymethyl-β-cyclodextrin conjugated magnetic nanoparticles as nano-adsorbents for removal of copper ions: synthesis and adsorption studies, J. Hazard. Mater., 185 (2011) 1177–1186.
[45] J. Pal, M.K. Deb, D.K. Deshmukh, D. Verma, Removal of methyl orange by activated carbon modified by silver nanoparticles, Appl. Water Sci., 3 (2013) 367–374.
[46] X.L. Wu, D.L. Zhao, S.T. Yang, Impact of solution chemistry conditions on the sorption behavior of Cu(II) on Lin'an montmorillonite, Desalination, 269 (2011) 84–91.
[47] Y.S. Ho, G. McKay, Pseudo-second order model for sorption processes, Process Biochem., 34 (1999) 451–465.
[48] Y.S. Ho, A.E. Ofomaja, Pseudo-second-order model for lead ion sorption from aqueous solutions onto palm kernel fiber, J. Hazard. Mater., 129 (2006) 137–142.
[49] J.P. Simonin, On the comparison of pseudo-first order and pseudo-second order rate laws in the modeling of adsorption kinetics, Chem. Eng. J., 300 (2016) 254–263.
[50] B. Noroozi, G.A. Sorial, H. Bahrami, M. Arami, Equilibrium and kinetic adsorption study of a cationic dye by a natural adsorbent-silkworm pupa, J. Hazard. Mater., 139 (2007) 167–174.
[51] S. Xu, J. Wang, R. Wu, J. Wang, H. Li, Adsorption behaviors of acid and basic dyes on crosslinked amphoteric starch, Chem. Eng. J., 117 (2006) 161–167.
[52] A. Gücek, S. Şener, S. Bilgen, M.A. Mazmancı, Adsorption and kinetic studies of cationic and anionic dyes on pyrophyllite from aqueous solution, J. Colloid Interface Sci., 286 (2005) 53–60.
[53] G. Crini, F. Gimbert, C. Robert, B. Martel, O. Adam, N. Morin-Crini, F. De Giorgi, P.M. Badot, The removal of Basic Blue 3 from aqueous solutions by chitosan-based adsorbent: batch studies, J. Hazard. Mater., 153 (2008) 96–106.
[54] F.K. Bangash, A. Manaf, Dyes removal from aqueous solution using wood activated charcoal of *Bombax cieba* tree, J. Chin. Chem. Soc., 52 (2005) 489–494.
[55] G. Zhang, S. Shuang, C. Dong, J. Pan, Study on the interaction of methylene blue with cyclodextrin derivatives by absorption and fluorescence spectroscopy, Spectrochim. Acta, Part A, 59 (2003) 2935–2941.
[56] G. Newcombe, M. Drikas, Adsorption of NOM activated carbon: electrostatic and non-electrostatic effects, Carbon, 35 (1997) 1239–1250.
[57] G. Alberghina, R. Bianchini, M. Fichera, S. Fisichella, Dimerization of Cibacron Blue F3GA and other dyes: influence of salts and temperature, Dyes Pigm., 46 (2000) 129–137.
[58] J. Germán-Heins, M. Flury, Sorption of Brilliant Blue FCF in soils as affected by pH and ionic strength, Geoderma, 97 (2000) 87–101.
[59] X. Peng, Z. Luan, H. Zhang, Montmorillonite-Cu(II)/Fe(III) oxides magnetic material as adsorbent for removal of humic acid and its thermal regeneration, Chemosphere, 63 (2006) 300–306.
[60] M.A. Fontecha-Cámara, M.V. López-Ramón, M.A. Álvarez-Merino, C. Moreno-Castilla, Effect of surface chemistry, solution pH, and ionic strength on the removal of herbicides diuron and amitrole from water by an activated carbon fiber, Langmuir, 23 (2007) 1242–1247.
[61] Y.Q. Hu, T. Guo, X.S. Ye, Q. Li, M. Guo, H.N. Liu, Z.J. Wu, Dye adsorption by resins: effect of ionic strength on hydrophobic and electrostatic interactions, Chem. Eng. J., 228 (2013) 392–397.
[62] A. Shukla, Y.H. Zhang, P. Dubey, J.L. Margrave, S.S. Shukla, The role of sawdust in the removal of unwanted materials from water, J. Hazard. Mater., 95 (2002) 137–152.
[63] S.T. Yang, X.M. Ren, G.X. Zhao, W.Q. Shi, G. Montavon, B. Grambow, X.K. Wang, Competitive sorption and selective sequence of Cu(II) and Ni(II) on montmorillonite: batch, modeling, EPR and XAS studies, Geochim. Cosmochim. Acta, 166 (2015) 129–145.
[64] F. Renault, N. Morin-Crini, F. Gimbert, P.M. Badot, G. Crini, Cationized starch-based material as anew ion-exchanger adsorbent for the removal of C.I. Acid Blue 25 from aqueous solutions, Bioresour. Technol., 99 (2008) 7573–7586.
[65] M. Greluk, Z. Hubicki, Efficient removal of Acid Orange 7 dye from water using the strongly basic anion exchange resin Amberlite IRA-958, Desalination, 278 (2011) 219–226.
[66] M. Wawrzkiewicz, Removal of C.I. Basic Blue 3 dye by sorption onto cation exchange resin, functionalized and non-functionalized polymeric sorbents from aqueous solutions and wastewaters, Chem. Eng. J., 217 (2013) 414–425.